

# Features of $\omega$ photoproduction off proton target at backward angles : Role of nucleon Reggeon in $u$ -channel with parton contributions

Byung-Geel Yu\* and Kook-Jin Kong†

*Research Institute of Basic Science, Korea Aerospace University, Goyang, 10540, Korea*

Backward photoproduction of  $\omega$  off a proton target is investigated in a Reggeized model where the  $u$ -channel nucleon Reggeon is constructed from the nucleon Born terms in a gauge invariant way. The  $t$ -channel meson exchanges are considered as a background. While the  $N_\alpha$  trajectory of the nucleon Reggeon reproduces the overall shape of NINA data measured at the Daresbury Laboratory in the range of  $u$ -channel momentum transfer squared  $-1.7 < u < 0.02 \text{ GeV}^2$  and energies at  $E_\gamma = 2.8, 3.5$  and  $4.7 \text{ GeV}$ , a possibility of parton contributions is searched for through the nucleon isoscalar form factor which is parameterized in terms of parton distributions at the  $\omega NN$  vertex. Detailed analysis is presented for NINA data to understand the reaction mechanism that could fill up the deep dip from the nucleon Reggeon at momentum squared  $u = -0.15 \text{ GeV}^2$ . The angle dependence of differential cross sections at the NINA energies above are reproduced in the overall range of  $u$  including the CLAS data at forward angles in addition. The energy dependence of the differential cross section is investigated based on the NINA data and the recent LEPS data. A feature of the present approach that implicates parton contributions via nucleon form factor is illustrated in the total and differential cross sections provided by GRAAL and CB-ELSA Collaborations.

PACS numbers: 11.55.Jy, 13.40.-f, 13.60.Le, 12.38.-t

## I. INTRODUCTION

Understanding the structure of hadrons based on QCD is a longstanding issue and hadron reactions at wide angles are useful means to investigate parton contributions to reaction processes. In search of parton distributions in hadrons the recent experimental activities and theoretical developments have been concentrated on identifying the scaling of cross sections for meson photo/electroproductions at mid angle [1–5] as well as the hadron form factors in terms of parton densities at large virtual photon momentum squared [6–8].

In photoproductions of lighter vector mesons  $\rho$ ,  $\omega$ , and  $\phi$ , the peripheral scattering of mesons and Pomeron exchanges is suppressed at large angles, but an enhancement of quark exchange is expected due to the smaller impact parameter  $\sim 1/\sqrt{-t}$ . Scaling of differential cross sections for hadron reactions with respect to energy is one of the examples that perturbative QCD predicts at mid angle  $\theta \approx 90^\circ$  [1]. Possibilities of such hard processes were examined in the CLAS experiment where the differential cross sections of  $\omega$  photoproduction were measured over the resonance region  $2.6 < W < 2.9 \text{ GeV}$  up to a momentum transfer squared  $-t = 5 \text{ GeV}^2$  [9]. Around the mid angle  $\theta \approx 90^\circ$  the scaling of cross sections by  $s^8$  in the photon energy  $E_\gamma = 3.38 - 3.56 \text{ GeV}$  seem to be consistent with quark and gluon exchanges predicted by the QCD-inspired model [10] as well as the Reggeized meson exchanges in the  $t$ -channel with the trajectory saturated at large  $-t$  [11–14].

At very backward angles  $\theta \approx 180^\circ$  beyond resonances, however, theory and experiment in this kinematical re-

gion are rare [9, 10, 15–18] and only the data from the NINA electron synchrotron at the Daresbury Laboratory [17] are available at present for the  $u$ -channel momentum squared  $-1.8 < u < 0.02 \text{ GeV}^2$  at  $E_\gamma = 2.8 - 4.7 \text{ GeV}$ . Because of the isoscalar nature of  $\omega$  meson it is expected that the reaction at backward angles is dominated by the  $u$ -channel nucleon exchange with a dip at  $u = -0.15 \text{ GeV}^2$  arising from the nonsense wrong signature zero (NWSZ) of the  $N_\alpha$  trajectory. Interestingly enough, however, the measured cross section exhibited the dip much weaker than predicted by the Regge theory, and hence, a sort of a mechanism is needed to fill up the depth of the dip. While there are no other baryon trajectories to play such a role, the authors of Ref. [17] suggested a possibility of parton contributions there by showing the  $s^8$  scaling of cross section over the dip in the analysis of data at  $E_\gamma = 3.5 \text{ GeV}$ .

Recently this issue was reexamined in Ref. [15] to investigate backward  $\omega$  photoproduction in the baryon pole model with hadron form factors considered. However, the discussion on the reaction mechanism around the expected dip as well as its appearance in the data was no longer valid in the model, because the occurrence of a dip is a unique feature of the baryon trajectory at the NWSZ in the Regge theory. Thus, the production mechanism of  $\omega$  photoproduction at very backward angles remains not fully understood yet, and the topic raised by the NINA data should be revisited within the Regge framework for the  $u$ -channel nucleon exchange.

In this work we study backward  $\omega$  photoproduction with our interest in the search of hard process [10] involved in the NINA data [17]. Meanwhile, as the scaling of cross section for meson photoproduction is mostly due to quark and gluon dynamics through hard process in the midst of meson and baryon degrees of freedom [2, 3], it becomes, therefore, an important issue how to consider

\* bgyu@kau.ac.kr

† kong@kau.ac.kr

parton contributions in the hadronic amplitude of the Regge theory for the present process.

With these in mind, our purpose here is to find a way of considering parton distributions within the Regge framework for an understanding of parton contributions to the isotropic cross sections of NINA data observed in the very backward region.

This paper is organized as follows; Section II devotes to a construction of photoproduction amplitude where the nucleon exchange is reggeized with the background contribution from the meson exchanges. Discussion is given on how to consider parton contributions in the hadronic production amplitude. In Sec. III numerical consequences in the differential cross sections are presented to compare with existing data. More proofs for the validity of the present approach to current issue are given in the differential and total cross sections in the region where the nucleon Reggeon plays a role. Summary and discussions follow in Sec. IV.

## II. BARYON REGGEON MODEL

At backward angles where the  $u$ -channel momentum squared  $|u|$  is small hadron reactions are well described by the  $u$ -channel baryon Reggeon in the resonance region [19]. In this section we discuss a construction of photoproduction amplitude for the nucleon Reggeon because the isoscalar  $\omega$  prohibits baryon resonances of isospin  $I = 3/2$  from the  $\gamma p \rightarrow \omega p$  reaction. In the reggeization of the relativistic Born terms the nucleon exchange in the  $u$ -channel alone is not gauge invariant due to the charge coupling term and the nucleon exchange in the  $s$ -channel is introduced further to preserve gauge invariance of the production amplitude.

At higher energies beyond the resonance region, the meson exchange in the  $t$ -channel begins to give a contribution. To reproduce experimental data in the overall range of energy and angle, therefore, it is necessary to include the meson exchange as a background contribution. However, in order to avoid the possibility of double counting caused by the  $s$  and  $t$ -channel duality, if the  $t$ -channel is reggeized further in addition to the duality between  $s$  and  $u$ -channel by the  $u$ -channel Reggeon, we consider the  $t$ -channel meson exchanges in the pole model with the cutoff functions for the divergence of cross sections at high energies.

### A. Nucleon exchange reggeized in the $u$ -channel

For gauge invariance of nucleon exchange, as shown in Fig. 1, we now write the nucleon Born terms as

$$M_s = \bar{u}(p') \Gamma_{\omega NN} \frac{\not{p} + \not{k} + M_N}{s - M_N^2} \Gamma_{\gamma NN} u(p), \quad (1)$$

$$M_u = \bar{u}(p') \Gamma_{\gamma NN} \frac{\not{p}' - \not{k} + M_N}{u - M_N^2} \Gamma_{\omega NN} u(p), \quad (2)$$

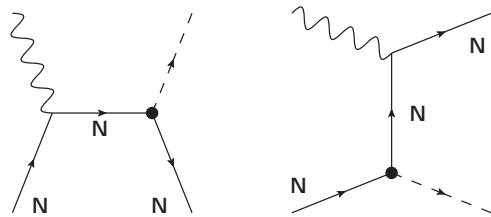


FIG. 1. Nucleon Born terms in  $s$ - and  $u$ -channels. Blobs at the  $\omega NN$  vertices indicate inclusion of the nucleon isoscalar form factor in addition to the point coupling interaction in Eq. (14).

where the electromagnetic and strong coupling vertices are given by

$$\Gamma_{\gamma NN} = e \left( e_N \not{\epsilon} - \frac{\kappa_N}{4M_N} [\not{\epsilon}, \not{k}] \right), \quad (3)$$

$$\Gamma_{\omega NN} = g_{\omega NN} \left( \not{\eta}^* + \frac{\kappa_\omega}{4M_N} [\not{\eta}^*, \not{q}] \right), \quad (4)$$

where  $u(p)$ ,  $\bar{u}(p')$  are Dirac spinors of the initial and final nucleons with momenta  $p$  and  $p'$ , and  $\epsilon^\mu$  and  $\eta^{\nu*}$  are polarization vectors of incoming photon and outgoing  $\omega$  with momenta  $k$  and  $q$ . Charge and anomalous magnetic moment are  $e_N = 1$ ,  $\kappa_N = 1.79$  for proton and  $e_N = 0$ ,  $\kappa_N = -1.91$  for neutron. We take  $g_{\omega NN} = 15.6$  by the universality of  $\omega$  meson decay constant  $f_\omega$ , and  $\kappa_\omega = 0$  for consistency with the results from other hadronic process  $\gamma N \rightarrow \pi^0 N$ , for instance [11].

The reggeization of the  $u$ -channel amplitude is simply done by replacing the  $u$ -channel pole ( $u - M^2$ ) with the nucleon Regge propagator  $\mathcal{R}^N(s, u)$ , and the reggeized amplitude is expressed as

$$\mathcal{M}_N = [M_s + M_u] \times (u - M_N^2) \mathcal{R}^N(s, u), \quad (5)$$

with  $\mathcal{R}^N(s, u)$  given by

$$\mathcal{R}^N(s, u) = \frac{\pi \alpha'_N}{\Gamma(\alpha_N(u) + 0.5)} \frac{(1 + \tau e^{-i\pi(\alpha_N(u) - 0.5)})}{2 \sin \pi(\alpha_N(u) - 0.5)} \times \left( \frac{s}{s_0} \right)^{\alpha_N(u) - 0.5}, \quad (6)$$

where the signature is defined as  $\tau = (-)^{J-1/2}$  and  $\tau = 1$  for nucleon.  $s_0 = 1 \text{ GeV}^2$ .

Given the baryon trajectory of the form for the spin  $J$

$$\alpha(\sqrt{u}) = \alpha' u + \alpha_0, \quad (7)$$

the MacDowell symmetry predicts the existence of the state with the same signature  $\tau$  but the opposite parity. Thus, denoting  $\alpha^+(\sqrt{u}) = \alpha^-(\sqrt{u})$  to distinguish the states between the same spin but opposite parities, the nonexistence of the parity negative state corresponding to the nucleon in the Chew-Frautschi plot should dictate  $1 + e^{-i\pi(\alpha_N(u)(\sqrt{u}) - 0.5)} = 0$  in order not to contribute to the reaction process, which leads to an occurrence of a dip with the NWSZ at some position of  $u$ .

In accordance with many applications we take the slope  $\alpha' = 0.9 \text{ GeV}^{-2}$ . But the value for the intercept  $\alpha_0$  in literature varies in the range around  $-0.3$ . Here, we choose  $\alpha_0 = -0.365$  so that the trajectory in Eq. (7) yields the dip at  $u = -0.15 \text{ GeV}^2$  measured in the NINA data at  $E_\gamma = 2.8, 3.5,$  and  $4.7 \text{ GeV}$  [17].

### B. Meson poles in $t$ -channel as a background

Now that the nucleon Reggeon in the  $u$ -channel in Eq. (5) gives the contribution, in general, by an order of magnitude smaller than that of the  $\pi$  exchange in the  $t$ -channel, it is not enough to reproduce the cross section data by the nucleon Reggeon contribution alone in the overall range of angles. Therefore, we consider the contribution of meson exchanges as a background on which the nucleon Reggeon is based. As discussed above we treat the meson exchange simply as the  $t$ -channel pole with a cutoff functions and cutoff masses.

For consistency with our previous work, we utilize the meson exchanges with coupling constants taken the same as in Ref. [14]. The meson exchanges in Ref. [14] are now given as the  $t$ -channel poles with the pole propagator,

$$(t - m_\varphi^2)^{-1} \quad (8)$$

and the cutoff function of the type

$$\left( \frac{\Lambda_\varphi^2 - m_\varphi^2}{\Lambda_\varphi^2 - t} \right)^n \quad (9)$$

for  $\varphi = \pi, \sigma,$  and  $f_1$ . As for the  $f_2$  exchange, however, due to the highly divergent behavior despite the large cutoff mass we regard it as the  $t$ -channel Reggeon together with the Pomeron exchange in Ref. [14]. To fix the cutoff mass  $\Lambda_\varphi$  in Eq. (9) we exploit the natural and unnatural parity cross sections over the resonance region. Before doing this, however, it should be cautioned that the determination of the sign of the  $\pi$  exchange relative to nucleon is of importance, because these two are the leading contributions to the reaction at forward and backward angles, respectively.

Given the nucleon Reggeon  $\mathcal{M}_N$  in Eq. (5) the production amplitude for the exchanges of the natural and unnatural parity mesons consists of the following two terms,

$$\mathcal{M}_{\text{nat.}} = \mathcal{M}_N + \mathcal{M}_\sigma + \mathcal{M}_{f_2} + \mathcal{M}_P, \quad (10)$$

$$\mathcal{M}_{\text{unnat.}} = \mathcal{M}_\pi + \mathcal{M}_{f_1}, \quad (11)$$

respectively.

In Fig. 2 (a) by adjusting the cutoff  $\Lambda_\sigma = 0.65 \text{ GeV}$  we find that the coupling constant  $g_{\omega NN} = +15.6$  gives a good fit to the natural parity cross section. By using  $\Lambda_{f_1} = 1.3 \text{ GeV}$  for  $f_1$  and  $\Lambda_\pi = 0.72 \text{ GeV}$  with  $n = 2$  to suppress the large coupling at  $\gamma\pi\omega$  vertex a fair agreement is obtained as shown in Fig. 2 (b). For further confirmation of the coupling constants and cutoff masses chosen above we will provide differential and total cross sections at low energies in the following section

TABLE I. Physical constants of exchanged mesons and parameters for form factors. Masses and cutoff parameters are given in units of MeV.  $f_2$  Reggeon and Pomeron are taken from Ref. [14].

Meson	Mass	$n$	$\Lambda_\varphi$	$g_{\gamma\varphi\omega}$	$g_{\varphi NN}$
$\pi$	134.977	2	720	-0.69	13.4
$\sigma$	500	1	650	-0.17	14.6
$f_1$	1281.9	1	1300	0.18	2.5

for numerical consequences. We summarize the coupling constants and cutoff masses in Table I.

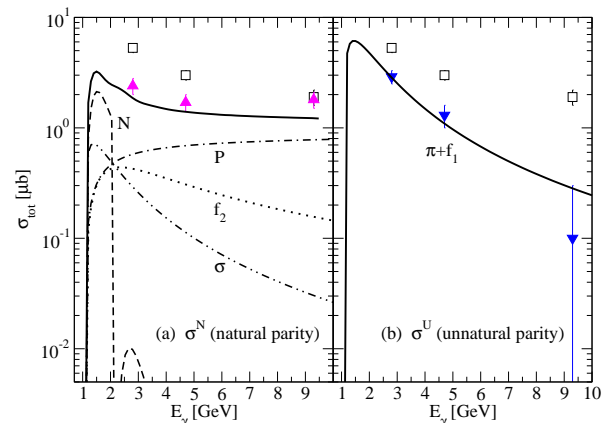


FIG. 2. Natural and unnatural parity cross sections for  $\gamma p \rightarrow \omega p$ . Dashed curve is from the proton Reggeon with a sequence of the dip from the  $N_\alpha$  trajectory.  $\kappa_p = 1.79, g_{\omega NN} = 15.6, \kappa_\omega = 0$  are taken in Eqs. (3) and (4). In (b) Solid curve is from  $\pi$  exchange with  $f_1$  of the  $10^{-5}$  order contribution. Data are taken from Ref. [20].

### C. Parton contribution and scaling

Since our interest is in the analysis of the reaction mechanism which is suggestive of the hard process at very small  $-u$ , we proceed to consider parton contributions in the hadronic amplitude in Eqs. (10) and (11).

The differential cross section for the  $u$ -channel momentum transfer squared is defined as

$$\frac{d\sigma}{du} = \frac{M_N^2}{16\pi(s - M_N^2)^2} \frac{1}{4} \sum_{\text{spins}} |\mathcal{M}|^2. \quad (12)$$

The NINA data from the reaction  $\gamma p \rightarrow \omega p$  at  $E_\gamma = 3.5 \text{ GeV}$  are analyzed by a parameterization of  $d\sigma/du$  which is divided by hadronic and hard scattering parts, respectively [17], i.e.,

$$\frac{d\sigma}{du} = \left| A(u)s^{\alpha(u)-1} + B(u)e^{i\phi(u)}s^{-n/2} \right|^2. \quad (13)$$

Then, a fit of data with the  $s^8$  scaling assumed in the hard scattering term produces the  $B(u)$  isotropic at the relative angle  $\phi \simeq 90^\circ$  for all  $u$ . This suggests incoherency between hadronic process and hard scattering [17]. More analysis [17] leads us to interpret the hadronic term as the Reggeon with energy dependence  $s^{\alpha-1}$ , in which case the trajectory  $\alpha(u)$  generates a typical dip at the expected position. The  $B(u)$  term in the hard scattering is regarded as parton contributions with  $s^8$  scaling with respect to the momentum squared  $u$ .

In order to include the parton contributions in the hadronic amplitude it is natural to suppose a possibility of parton distribution in nucleon form factors at very backward angles [7] in addition to the point coupling of  $\omega NN$  vertex in Eq. (4), as depicted in Fig. 2. For this we introduce the isoscalar form factor  $F^{(s)}(u)$  of the nucleon by the similarity of the  $\omega NN$  vertex to a virtual photon coupling,  $\gamma^* NN$ . Therefore, the  $\omega NN$  vertex in the nucleon Reggeon in Eq. (5) is extended to include the additional coupling, i.e.,

$$g_{\omega NN} \gamma^\nu \left( \frac{s}{s_0} \right)^{\alpha_N(u)} \rightarrow g_{\omega NN} \left[ \gamma^\nu \left( \frac{s}{s_0} \right)^{\alpha_N(u)} + e^{i\phi(u)} \gamma^\nu F^{(s)}(u) \left( \frac{s}{s_0} \right)^{\tilde{\alpha}_N(u)} \right] \quad (14)$$

with a relative angle  $e^{i\phi(u)}$  between the two coupling phases. As a result, the nucleon Reggeon is extended to include parton contributions via the nucleon isoscalar form factor,  $\mathcal{R}^N \rightarrow (\mathcal{R}^N + e^{i\phi(u)} F^{(s)}(u) \tilde{\mathcal{R}}^N)$ , and we write the full amplitude as

$$\mathcal{M} = (\mathcal{M}_N + \mathcal{M}_{\text{b.g.}}) + e^{i\phi} \tilde{\mathcal{M}}_N, \quad (15)$$

in accordance with Eq. (13) with the two terms in the first bracket referring to hadronic and the last to parton contributions, respectively. The term  $\mathcal{M}_{\text{b.g.}}$  represents the background coming from all the meson exchanges in the  $t$ -channel, i.e., all terms excluding the nucleon term  $\mathcal{M}_N$  in Eqs. (10) and (11). In the additional Reggeon  $\tilde{\mathcal{M}}_N$  which has the parton contributions via the form factor, we further assume that the nucleon trajectory  $\alpha_N(u)$  be modified to  $\tilde{\alpha}_N(u)$  in the presence of parton dynamics at very small  $|u|$ .

The relative angle  $e^{i\phi(u)}$  between hadronic and partonic phases is parameterized as a linear function of  $u$

$$\phi(u) = (au + b) \frac{\pi}{180} \quad (16)$$

with  $a$  in units of  $\text{GeV}^{-2}$ .

The nucleon isoscalar form factor is composed of proton and neutron charge form factors [21]

$$F^{(s)} = F_1^p + F_1^n, \quad (17)$$

and in the parton model the quark contents of these are expressed as

$$F_1^p = e_u u + e_d d, \quad F_1^n = e_u d + e_d u \quad (18)$$

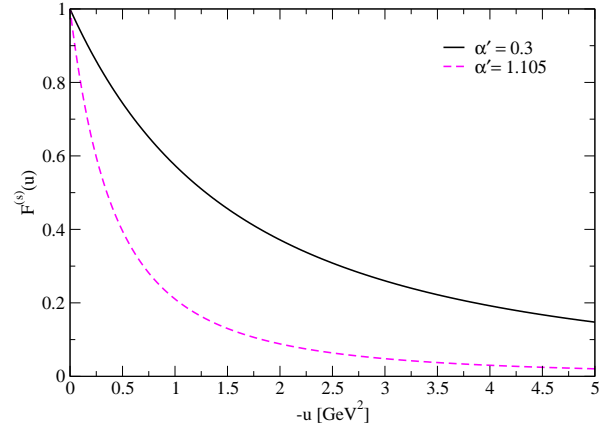


FIG. 3.  $u$  dependence of proton isoscalar form factor  $F^{(s)}(u)$ . Solid curve results from  $\alpha' = 0.3 \text{ GeV}^{-2}$  chosen for the present work and dashed curve from  $\alpha' = 1.105 \text{ GeV}^{-2}$  used for the fit of proton Dirac form factor  $F_1^p(Q^2)$  in the electroproduction  $p(\gamma^*, \pi^+ n)$  [7].

with the quark distribution [7]

$$q(u) = \int dx q_v(x) x^{-(1-x)\alpha'(u-u_0)} \quad (19)$$

for the valence quarks  $u$  and  $d$ . Here, we favor to choose the ansatz for the momentum fraction  $x$  dependence of partons which simulates the Regge trajectory with the slope  $\alpha'$  in units of  $\text{GeV}^{-2}$ , because of the relevance to the present formalism. The momentum squared  $u_0$  is the maximum value of  $u$  to avoid a rapid divergence in the region  $u > 0$  and  $\alpha'$  is considered to be a parameter chosen for calculation. As to the valence quark  $q_v(x)$  we employ the unpolarized parton distributions for  $u$  and  $d$  quarks which are

$$u_v = 0.262x^{-0.69}(1-x)^{3.5} (1 + 3.83x^{0.5} + 37.65x), \quad (20)$$

$$d_v = 0.061x^{-0.65}(1-x)^{4.03} (1 + 49.05x^{0.5} + 8.65x) \quad (21)$$

at the input scale  $\mu^2 = 1 \text{ GeV}^2$ , respectively. In the fitting procedure for the relative angle  $\phi(u)$  and the trajectory  $\tilde{\alpha}_N(u)$  to NINA data we make the slope parameter adjusted to obtain  $\alpha' = 0.3$  for a better result.

The sensitivity of proton isoscalar form factor  $F^{(s)}(u)$  to the slope parameter  $\alpha'$  is examined to discuss its implication to physical processes. In Fig. 3 the form factor with  $\alpha' = 0.3$  chosen here is compared to the case with  $\alpha' = 1.105$  that is obtained from the fit of proton Dirac form factor  $F_1^p$  to empirical data [22]. (We mean that the dependence of the form factor upon the momentum squared  $u$  is the same as the case upon the virtual photon momentum squared  $Q^2$ .) Giving the contribution stronger than the case with 1.105, as shown, the choice of  $\alpha' = 0.3$  largely deviates from the empirical form factor with  $\alpha' = 1.105$  for on-mass shell. In an application to hadron reactions just as the  $\omega$  photoproduction, however, in order to agree with the differential data at  $u = -0.15 \text{ GeV}^2$  the slope  $\alpha' = 0.3$  is favored rather than the case

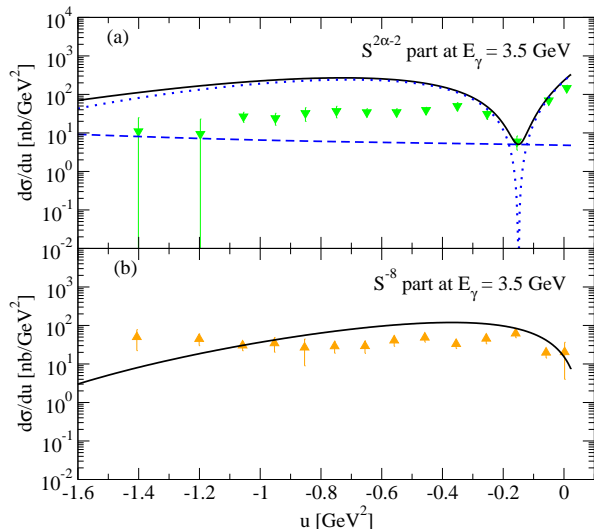


FIG. 4. Differential cross section for  $\gamma p \rightarrow \omega p$  at  $E_\gamma = 3.5$  GeV in accordance with Eq. (13). The curve in (a) results from the hadronic contribution consisting of the nucleon Reggeon,  $\mathcal{M}_N$  (dotted curve) with the  $t$ -channel meson-pole exchange,  $\mathcal{M}_{b.g.}$  (dashed). The curve in (b) which shows the scaling with respect to momentum squared  $u$  is resultant of  $\widetilde{\mathcal{M}}_N$  in Eq. (15) with  $\tilde{\alpha}_N = 0.9u - 0.56$  and the parton distributions in the  $F^{(s)}(u)$  form factor given in the text. Data are taken from Ref. [17].

of 1.105. This is similar to the proton Dirac form factor  $F_1^p(Q^2)$  in electroproduction  $\gamma^* p \rightarrow \pi^+ n$  [22], in which case the dipole fit of the form factor with the cutoff mass  $\Lambda = 1.55$  GeV is advantageous to agree with electroproduction data rather than the form factor with  $\alpha' = 1.105$ . Our choice of  $\alpha' = 0.3$  yields the form factor which lies between the dipole form factor above and the one prescribed by Kaskulov and Mosel [23]. We regard these results to be feasible, because the form factor in hadron reactions is, in general, half off-shell which need not be the same as the on-shell one.

### III. NUMERICAL RESULTS

In the fitting procedure to NINA data, our practical purpose is how to fill up such a deep dip as shown by the dotted curve that results from the nucleon Reggeon  $\mathcal{M}_N$  in Fig. 4 (a) and how to simulate the scaling behavior of the cross section with respect to the momentum squared  $u$  in (b) with parton contributions from the nucleon Reggeon  $\widetilde{\mathcal{M}}_N$  in addition. However, there is no evidence for a dip in the cross section of (b) for which the additional Reggeon  $\widetilde{\mathcal{M}}_N$  is applied, while it should produce a dip at the same place of  $u$  by the NWSZ of the trajectory  $\tilde{\alpha}_N(u)$ , unless different from the  $\alpha_N(u)$ . Thus, expecting not only the scaling without a dip in the hard scattering but also the reaction mechanism to fill up the depth of the original dip by a destructive inter-

ference between hadronic and hard processes, we have to move the position of the dip by  $\widetilde{\mathcal{M}}_N$  to another place by altering the trajectory  $\tilde{\alpha}_N$  in Eq. (14). Hence, we let the trajectory of the  $\widetilde{\mathcal{R}}^N$  vary in the fitting procedure to obtain

$$\tilde{\alpha}_N(u) = 0.9u - 0.56 \quad (22)$$

with the intercept adjusted for the best fit to the NINA data in the overall range of energy and angle. The dip position of  $\widetilde{\mathcal{R}}^N$  is now at  $u = +0.067$  GeV<sup>2</sup>, and hence, not appearing in the kinematical region of the reaction  $u < 0.02$  GeV<sup>2</sup> so that the resulting cross section in (b) could simulate the scaling without a dip, as shown by the solid curve.

Given the differential cross section  $d\sigma/du$  for  $\gamma p \rightarrow \omega p$  at  $E_\gamma = 3.5$  GeV separately into two parts as in Eq. (13), the hadronic contribution corresponding to the  $s^{\alpha(u)-1}$  term and the  $s^{-8}$  scaling by parton contributions are shown in Fig. 4 (a) and (b), respectively. In (a) the solid curve results from the sum of the dotted curve by the nucleon Reggeon and the dashed one by the  $t$ -channel meson exchanges, i.e., from the hadronic amplitude  $\mathcal{M}_N + \mathcal{M}_{b.g.}$  in Eq. (15). As expected, the Reggeon  $\mathcal{M}_N$  produces the deep dip at  $u = -0.15$  GeV<sup>2</sup> some part of which could be covered over with the meson contribution. Nevertheless, the dip remains not fully compensated yet. Moreover, the solid curve of the hadronic contributions  $\mathcal{M}_N + \mathcal{M}_{b.g.}$  is overestimating the data over  $0.3$  GeV<sup>2</sup>  $< |u|$ , which should be reduced. In (b) the solid curve is from the additional Reggeon,  $\widetilde{\mathcal{M}}_N$  with the trajectory  $\tilde{\alpha}_N(u) = 0.9u - 0.56$  with the dip at  $u = +0.067$  GeV<sup>2</sup> so that the  $\widetilde{\mathcal{M}}_N$  could preserve the cross section data without dip near  $u \approx 0$ . On the other hand, this term, when combined with the hadronic part  $\mathcal{M}_N + \mathcal{M}_{b.g.}$  via the relative angle  $\phi \simeq 90^\circ$ , should fill up the rest of the part of the dip as well as it should reduce the overestimating contribution of the solid curve to hadronic data in (a).

Figure 5 shows the differential cross section  $d\sigma/du$  for  $\gamma p \rightarrow \omega p$  when the cross sections (a) and (b) of Fig. 4 are combined with each other. The parameters  $a = -65$  and  $b = 93$  are chosen for the relative angle  $\phi(u)$  between hadronic and parton phase of the reaction process in Eq. (13). In actual, these parameters correspond to  $\phi = 0.57\pi$  at  $u = -0.15$  GeV<sup>2</sup> which is close to  $\phi \simeq 90^\circ$  from the decomposition of the NINA data in Fig. 3. The additional Reggeon  $\widetilde{\mathcal{M}}_N$  with parton contributions vanishes over  $|u| > 2$  GeV<sup>2</sup>. The respective roles of the Reggeon  $\mathcal{M}_N$  and the meson exchanges  $\mathcal{M}_{b.g.}$  in the  $t$ -channel are depicted by the dash-dotted and dash-dash-dotted curves in order. The rapid increase of cross sections in the NINA data at large  $|u|$  are identified by the  $t$ -channel meson exchanges, while the Reggeon  $\mathcal{M}_N$  gives the contribution in the backward region  $|u| < 2.5$  GeV<sup>2</sup>, as expected. We further note that these hadronic contributions,  $\mathcal{M}_N + \mathcal{M}_{b.g.}$  reproduce the shape convex up in the interval  $-3.5 < u < -2.5$  GeV<sup>2</sup> which was once described by the two quarks exchange in previous work

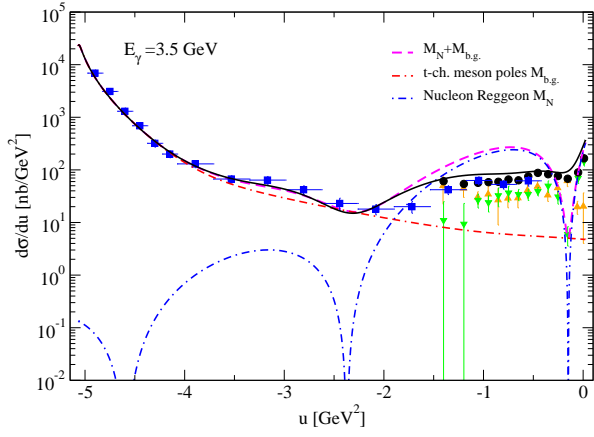


FIG. 5. Differential cross section for  $\gamma p \rightarrow \omega p$  at  $E_\gamma = 3.5$  GeV. The dashed curve corresponds to the solid one in Fig 4 (a). The solid curve from the full amplitude shows a good agreement with data in the overall range of  $u$  with the fit of  $a = -65$ ,  $b = 93$  for  $\phi(u)$ . Data are collected from Refs. [9] and [17].

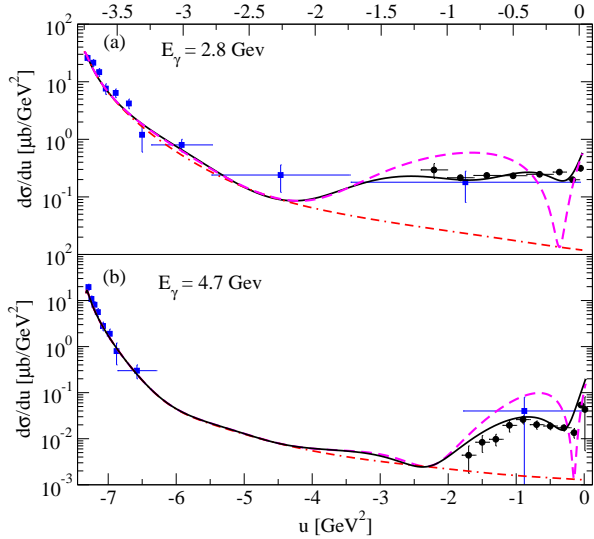


FIG. 6. Differential cross sections  $d\sigma/du$  at  $E_\gamma = 2.8$  and  $4.7$  GeV with the parton contributions in Eq. (15) included. The cross section in the upper panel is fitted with  $a = -95$ ,  $b = 70$  and lower with  $a = -35$ ,  $b = 120$  for  $\phi(u)$ . Notations are the same as in Fig. 5. Data are taken from Refs. [17, 20].

as elaborated in Ref. [10]. In the current approach since the dip position of  $\widetilde{\mathcal{R}}^N$  is removed out to the kinematical region, the term  $\widetilde{\mathcal{M}}_N$  could play the role to fill up some part of the original dip at  $u = -0.15$  GeV<sup>2</sup> as well as to reduce the overestimating contribution of the hadronic part (dashed curve) in Figs. 5 and 6 up to  $u \approx -2$  GeV<sup>2</sup>, when combined with each other through  $\phi \simeq 90^\circ$ .

Differential cross sections  $d\sigma/du$  at  $E_\gamma = 2.8$  and  $4.7$  GeV are presented in Fig. 6 to show a fair agreement with data. The cross section at  $E_\gamma = 2.8$  GeV in the upper panel is fitted with  $a = -95$  and  $b = 70$  and the cross

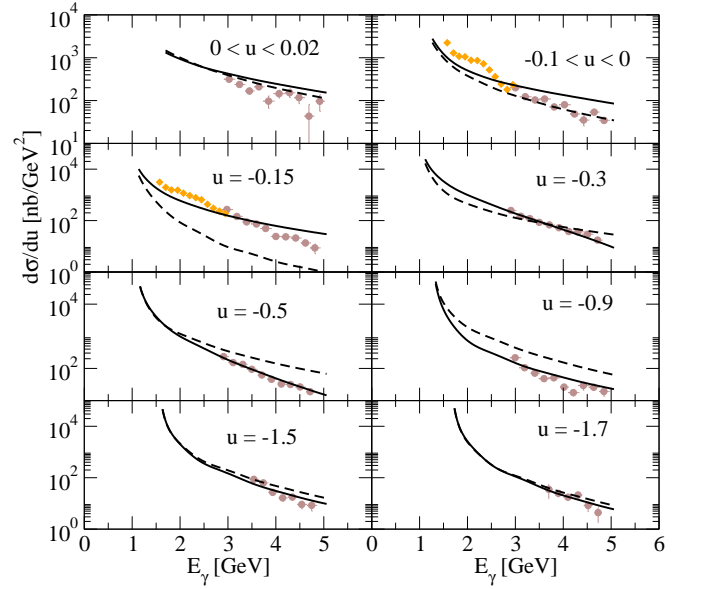


FIG. 7. Energy dependence of differential cross sections  $d\sigma/du$ . The solid curve is reproduced by a linear fit of data with  $a = 31\text{GeV}^{-1}E_\gamma - 178$  and  $b = 26\text{GeV}^{-1}E_\gamma - 0.64$  for the relative angle  $\phi$ . The dashed curve is without parton contributions. The momentum squared  $u$  is given in units of GeV<sup>2</sup>. Data over  $E_\gamma \approx 3$  GeV are taken from Ref. [17] and at low energies are taken from Ref. [18].

section in the lower panel with  $a = -35$  and  $b = 120$  for  $\phi$ , respectively. These parameters at  $u = -0.15$  GeV<sup>2</sup>, for instance, yield  $\phi \approx 0.47\pi$  and  $\phi \approx 0.7\pi$ , in order. Thus, the relative angle  $\phi$  is not quite unique to energy dependence of cross sections and we have to change the parameters  $a$  and  $b$  to accomplish such an agreement with data at the photon energies  $E_\gamma = 2.8, 3.5$ , and  $4.7$  GeV given. The contribution of meson exchanges as shown by the dash-dash-dotted curve is responsible for the forward enhancement of the cross section at large  $|u|$ , as before. Solid curve shows the improvement of hadronic contribution (dashed curve) by the additional Reggeon  $\widetilde{\mathcal{M}}_N$  with parton contributions at backward angles.

To test the validity of the present approach further we check up the energy dependence of differential cross sections in the range  $-1.8 < u < 0.02$  GeV<sup>2</sup> and present the result in Fig. 7. The NINA cross sections  $d\sigma/du$  in eight angle bins are reproduced up to photon energy  $E_\gamma = 5$  GeV. In the differential cross sections at  $-0.1 < u < 0$  and  $u = -0.15$  GeV<sup>2</sup> the data recently measured at the SPring-8/LEPS facility [18] are included further for relevance to the present analysis. Since the angle  $\phi$  has the energy dependence as shown in Figs. 5 and 6, we make parameterized  $a = 31\text{GeV}^{-1}E_\gamma - 178.2$  and  $b = 26\text{GeV}^{-1}E_\gamma - 0.64$  for  $\phi$  as a linear function of photon energy. It is interesting to see the peculiar behavior of the cross section at  $u = -0.15$  GeV<sup>2</sup>. The difference between the contributions of nucleon Reggeon with and without partons via the form factor  $F^{(s)}$  becomes max-

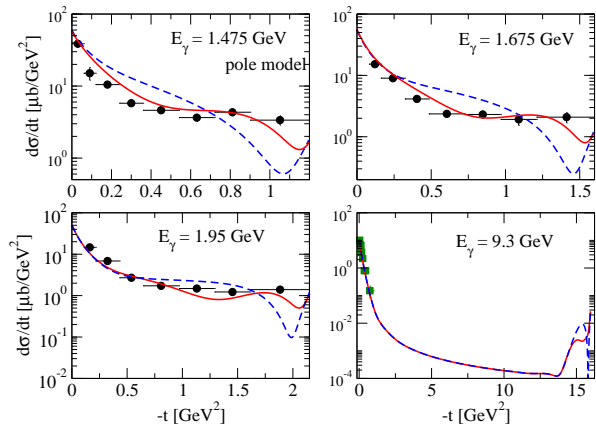


FIG. 8. Differential cross sections for  $\gamma p \rightarrow \omega p$  in low energy region below  $E_\gamma = 2$  GeV and at high energy  $E_\gamma = 9.3$  GeV. Solid curves are from the full calculation with parton contributions. Dashed curves are without parton contributions. Data below 2 GeV are taken from Ref. [24] and data at 9.3 GeV from Ref. [20].

imal around the dip position at  $u = -0.15$  GeV<sup>2</sup> and vanishes over  $u \approx -1.7$  GeV<sup>2</sup>, as expected. With an expectation that the exponent  $x$  of  $As^{-x}$  term converted to an effective trajectory  $\alpha(u)$ , as indicated in Ref. [17], the role of new trajectory  $\tilde{\alpha}_N(u)$  with parton contributions is significant at  $u = -0.15$  GeV<sup>2</sup>, although we do not follow the negative power of  $x$  assumed there. The analysis of Fig. 7 is consistent with the observation of Ref. [17] that the slope of the cross section at  $u = -0.15$  GeV<sup>2</sup> is different from others. We obtain a reasonable result in cross sections that cover the overall range of energy and momentum of NINA data. These findings further support the validity of the present approach.

Predictions for differential and total cross sections are presented in Figs. 8 and 9 with the parameters  $a$  and  $b$  in Fig. 7 for the angle  $\phi$ . The differential cross sections are reproduced in the overall range of  $-t$  at the given energy  $E_\gamma$ . In Fig. 8 each cross section at very backward angles reveals the role of the nucleon isoscalar form factor with partons to make the model prediction closer to experimental data even in the low energy region less than  $E_\gamma = 2$  GeV. Within the present framework it is rather natural that parton contributions via the form factor could appear at lower energies where the nucleon Reggeon is dominant. Such an evidence of parton distributions at low energies can be traced out in the total cross section as presented up to  $E_\gamma = 6$  GeV in Fig. 9. The nucleon isoscalar form factor with parton distributions plays the role to reduce the cross section. Thus, it is a feature of the present approach that the parton distribution could play a role through hadron form factors without deep scattering of virtuality photon at high energies. Together with nucleon Reggeon, a fair agreement with data on total and differential cross sections further confirms the validity of the background contribution with cutoff masses chosen for the present calculation.

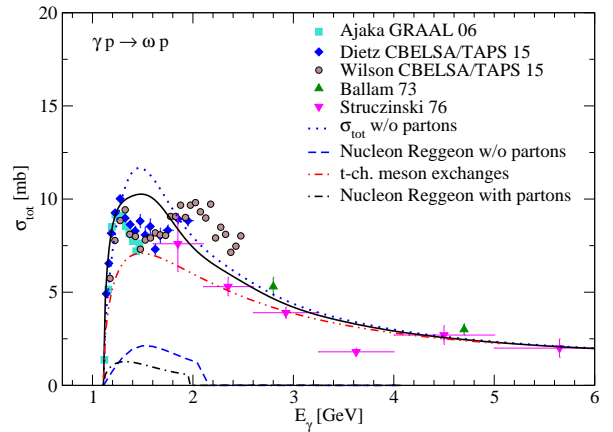


FIG. 9. Total cross section for  $\gamma p \rightarrow \omega p$ . Cross sections  $\sigma_{tot}$  with and without parton contributions are given by solid and dotted curves in response to the nucleon contributions with and without isoscalar form factor which are given by dashed and dash-dotted curves. The background contribution from the  $t$ -channel exchange is depicted by dash-dot-dotted curve. Data are taken from Refs. [20, 24–27].

#### IV. SUMMARY AND DISCUSSIONS

Backward photoproduction of  $\omega$  meson off a proton target is investigated within the Regge framework where the nucleon Born terms in the  $s$ - and  $u$ -channels are reggeized for the gauge invariant  $u$ -channel nucleon Reggeon. The exchanges  $\sigma + \pi + f_1 + f_2 + Pomeron$  in the  $t$ -channel are included as a background contribution to reproduce reaction cross sections. The cutoff masses for the cutoff functions for  $\sigma + \pi + f_1$  poles in the  $t$ -channel are determined from natural and unnatural parity cross sections as shown in Fig. 2.

While the  $N_\alpha$  trajectory of the nucleon Reggeon reproduces the overall shape of the NINA data measured at the Daresbury Laboratory in the range of  $-1.7 < u < 0.02$  GeV<sup>2</sup> and energies at  $E_\gamma = 2.8, 3.5$  and  $4.7$  GeV, a possibility of parton contributions is searched for by considering the nucleon isoscalar form factor at the  $\omega NN$  vertex which is parameterized in terms of parton distributions. The nucleon Reggeon would make a deep dip at  $u = -0.15$  GeV<sup>2</sup>, which should be covered over by a fill-up mechanism in order to agree with the cross sections observed in the Daresbury experiment. The dip of the nucleon Reggeon is covered over partly with the meson exchanges and partly with the additional Reggeon with partons at very small  $|u|$ . From the practical point of view a manipulation of the relative phase  $\phi \simeq 90^\circ$  and the need of the  $t$ -channel contributions are of importance to reproduce the NINA data. Due to the parton densities in the nucleon isoscalar form factor, the parton contributions through the nucleon Reggeon activates rather in the lower energy region than is usually expected, as shown by the description of total and differential cross sections of GRAAL and CB-ELSA Collaborations.

Confronting the impending 12 GeV upgrade of CLAS detector, it is timely interesting to observe in experiments how partons would manifest themselves in the midst of hadronic degrees of freedom and how we could understand such a phenomenology through theoretical analysis. In this work we have illustrated how to incorporate parton distributions with hadronic degrees of freedom in hadron models just as the Regge model and the prescription we favored here offers an intuitive way to consider parton contributions in hadron reactions via the hadron form factors. Together with the scaling of meson photo-production by the factor  $s^7$  around mid angle  $\theta = 90^\circ$  observed in the Jefferson Lab, the NINA data at Daresbury,

though almost a 30 years-old issue, provide information further for our understanding of quark dynamics inside hadrons in the limit  $-u \approx 0$  that we could expect to observe in future experiments at the 12 GeV upgraded CLAS as well as those facilities LEPS, CB-ELSA, and GRAAL.

## ACKNOWLEDGMENTS

This work was supported by the National Research Foundation of Korea Grant No. NRF-2017R1A2B4010117.

- 
- [1] S. J. Brodsky and G. R. Farrar, Phys. Rev. Lett. **31**, 1153 (1973).
- [2] H. W. Huang, R. Jakob, P. Kroll, and K. Passek-Kumericki, Eur. Phys. J. C **33**, 91 (2004).
- [3] S. V. Goloskokov and P. Kroll, Eur. Phys. J. C **42**, 281 (2005).
- [4] B. Dey, Phys. Rev. D **90**, 014013 (2014).
- [5] L. Y. Zhu *et al.*, Phys. Rev. Lett. **91**, 022003-1 (2003).
- [6] T. Horn *et al.*, Phys. Rev. Lett. **97**, 192001 (2006).
- [7] M. Guidal, M. V. Polyakov, A. V. Radyushkin, and M. Vanderhaeghen, Phys. Rev. D **72**, 054013 (2005).
- [8] M. Diehl and P. Kroll, Eur. Phys. J. C **73**, 2397 (2013).
- [9] M. Battaglieri *et al.* (CLAS Collaboration), Phys. Rev. Lett. **90**, 022002-1 (2003).
- [10] J.-M. Laget, Phys. Lett. B **489**, 313 (2000).
- [11] K.-J. Kong, T. K. Choi, and B.-G. Yu, Phys. Rev. C **94**, 025202 (2016).
- [12] B.-G. Yu, Hungchong Kim, and K.-J. Kong, Phys. Rev. D **95**, 014020 (2017).
- [13] B.-G. Yu and K.-J. Kong, Phys. of Part. and Nucl. Lett. **15**, 438 (2018); arXiv:1709.08175/hep-ph.
- [14] B.-G. Yu and K.-J. Kong, arXiv:1710.04511/hep-ph.
- [15] A. Sibirtsev, K. Tsushima, S. Krewald, arXiv:nucl-th/0202083
- [16] B. Pire, K. Semenov-Tian-Shansky and L. Szymanowski, Phys. Rev. D **91**, 094006 (2015).
- [17] R. W. Clift *et al.*, Phys. Lett. B **72**, 144 (1977).
- [18] Y. Morino *et al.*, Prog. Theor. Exp. Phys. 013D01, (2015).
- [19] M. Guidal, J.-M. Laget, M. Vanderhaeghen, Nucl. Phys. A **627**, 645 (1997).
- [20] J. Ballam, G. B. Chadwick, Y. Eisenberg, E. Kogan, K. C. Moffeit, P. Seyboth, I. O. Skillicorn, H. Spitzer, G. Wolf, H. H. Bingham, W. B. Fretter, W. J. Podolsky, M. S. Rabin, A. H. Rosenfeld, and G. Smadja, Phys. Rev. D **7**, 3150 (1973).
- [21] C. F. Perdrisat, V. Punjabi, and M. Vanderhaeghen, Prog. Part. Nucl. Phys. **59**, 694 (2007).
- [22] T. K. Choi, K.-J. Kong, B.-G. Yu, J. of Kor. Phys. Soc. **67**, 1089 (2015), arXiv:1508.00969v4 [nucl-th].
- [23] M. M. Kaskulov and U. Mosel, Phys. Rev. C **81**, 045202 (2010).
- [24] F. Dietz *et al.* (CB-ELSA/TAPS Collaboration), Eur. Phys. A **51**, 6 (2015).
- [25] A. Wilson *et al.* (CB-ELSA/TAPS Collaboration), Phys. Lett. B **749**, 407 (2015).
- [26] J. Ajaka, Y. Assafri, S. Bouchigny, J. P. Didelez, L. Fichen, M. Guidal, E. Hourany, V. Kouznetsov, R. Kunne, A. N. Mushkarenkov, V. Nedorezov, N. Rudnev, A. Turling, and Q. Zhao, Phys. Rev. Lett. **96**, 132003 (2006).
- [27] W. Struczinski *et al.* (AHHM Collaboration), Nucl. Phys. B **108**, 45 (1976).